
In What Ways Are Deep Neural Networks Invariant and How Should We Measure This?

Henry Kvinge^{1,2}, Tegan H. Emerson^{1,3,4}, Grayson Jorgenson¹,
Scott Vasquez¹, Timothy Doster¹, Jesse D. Lew⁵

¹Pacific Northwest National Laboratory

²Department of Mathematics, University of Washington

³Department of Mathematics, Colorado State University

⁴Department of Mathematical Sciences at the University of Texas, El Paso

⁵National Geospatial-Intelligence Agency

henry.kvinge@pnnl.gov

Abstract

It is often said that a deep learning model is “invariant” to some specific type of transformation. However, what is meant by this statement strongly depends on the context in which it is made. In this paper we explore the nature of invariance and equivariance of deep learning models with the goal of better understanding the ways in which they actually capture these concepts on a formal level. We introduce a family of invariance and equivariance metrics that allows us to quantify these properties in a way that disentangles them from other metrics such as loss or accuracy. We use our metrics to better understand the two most popular methods used to build invariance into networks: data augmentation and equivariant layers. We draw a range of conclusions about invariance and equivariance in deep learning models, ranging from whether initializing a model with pretrained weights has an effect on a trained model’s invariance, to the extent to which invariance learned via training can generalize to out-of-distribution data.

1 Introduction

The notions of invariance and equivariance have been guiding concepts across a diverse range of scientific domains, from physics to psychology. In machine learning (ML) the concept of invariance is frequently invoked to describe models whose output does not change when its input is transformed in ways that are irrelevant to the task the model was designed for. For a dog or cat image classifier, for example, it is desirable for the model to be reflection invariant so that the same prediction is made whether or not the input image is reflected across its vertical axis. This type of invariance is useful in this model because although an image generally changes when reflected, whether it contains a dog or cat does not. Equivariance is used to describe models whose output changes in a manner that is aligned with the way that input is transformed. For example, as an image is rotated, the position of bounding boxes predicted by an object detector should also rotate (thus, the object detector should be rotation equivariant).

While mathematicians have developed rigorous theory that can describe invariance and equivariance, the amount of this that is actually used in the context of ML varies dramatically among different works. Within computer vision, research on relatively simple image transformations (i.e., rotations or translations) is often presented within a solid group-theoretic framework [6; 52; 9]. Other work dealing with more complex types of transformations such as changes in image background have (by necessity) needed to be more informal [51]. Furthermore, while model invariance and equivariance are frequently a central component in a broad range of ML research, limited effort has been put

into trying to measure them directly with the purpose of understanding the general invariance and equivariance properties of deep learning models. Rather, most works measure them indirectly through other ML metrics that align with the ultimate purpose of the model (e.g., loss or accuracy). While such a strategy makes sense when optimizing model performance is the primary objective, we miss an opportunity to better understand how and why deep neural networks work (or fail). The purpose of this paper is to propose a group-theoretic family of metrics, associated to an arbitrary group of symmetries G , which we call *G -empirical equivariance deviation (G -EED)*, that quantify the G -equivariance (and G -invariance) of a model.

Informally, the G -EED of a model measures the extent to which it fails to be G -equivariant on a specific data distribution and with respect to a specific notion of distance in output space. This aligns with needs in ML where the user of a model may care only that their model is equivariant on data that the model will actually encounter in practice and not on any possible input. Further, since invariance is a special case of equivariance, G -EED also measures the extent to which a model fails to be invariant to the action of G . To show the breadth of the G -EED concept, we give a number of different ways it can be applied to measure different aspects of equivariance in a model. For example, we show how G -EED can be applied to a model’s latent space representations to measure the extent to which a model extracts G -invariant features.

Finally, we use G -EED to answer a range of questions about invariance and equivariance in neural networks, with a focus on the two most popular ways of inducing invariance in these models: data augmentation and equivariant architectures. Some of the conclusions we draw from our experiments include the following. (1) Training with augmentation does not tend to induce invariance through learned equivariant layers; rather, invariance arises through some other mechanism. (2) Invariance learned through augmentation does generalize mildly to out-of-distribution data (e.g., common image corruptions), but apparent invariance seen for far out-of-distribution data (e.g., images from a completely different domain) could be the result of model insensitivity. (3) Invariance should not be assumed to correlate with model performance: models with random weights can be more invariant (in the usual mathematical sense) than models with learned or hard-coded invariance. (4) Models initialized with pretrained weights tend to have different invariance or equivariance properties than models initialized with random weights though whether these models are judged to be more invariant depends on the specific notion of distance one chooses to use. (5) Self-supervised models do not seem to be more invariant than supervised models except when they are trained with contrastive loss and augmentations from the relevant symmetry group G .

In summary, the contributions of this paper include:

- The introduction of G -empirical equivariance deviation, the first family of metrics that can rigorously and directly measure a range of notions of invariance and equivariance in deep learning models.
- A demonstration of the flexibility of G -EED, showing that it can be applied easily to a range of different components of a deep learning model to measure different forms of invariance and equivariance.
- Use of G -EED to answer a range of questions, shedding light on the extent to which neural networks are or are not invariant and equivariant.

2 Related Work

The literature on invariance and equivariance in machine learning can roughly be partitioned into two groups: those works that focus on how to build invariance and equivariance into a model or its components [27; 9; 52; 45; 10; 46; 19; 12; 37; 41; 2] and those works that focus on the theory behind invariance and equivariance [3; 6; 5; 34; 40].

Three common approaches are used to build invariance into deep learning models: data augmentation, feature averaging, and equivariant architectures. In this paper we focus on the first and third of these. Outside of a few ubiquitous layer types (such as standard translation equivariant convolutional layers), data augmentation is by far the most commonly used method, being a standard component of many training routines, particularly in computer vision. Since it has become a common procedure when training deep learning models, data augmentation research has expanded in many directions [12; 37; 41; 2].

The idea that G -invariance can be hardcoded into a model by combining multiple G -equivariant layers with data reduction layers (e.g., pooling) has a long history in deep learning. The most famous example of this idea is the conventional convolutional neural network (CNN) [32]. Since then a multitude of other group equivariant layers have been designed including two-dimensional rotation equivariant layers [47; 50; 36; 38; 39], three-dimensional rotational equivariant layers [46; 11; 16], layers equivariant to the Euclidean group and its subgroups [45] (which we test against in this paper), and layers that are equivariant with respect to the symmetric group [33].

Our work is not the first to analyze various aspects of invariance in neural network models. Lyle et al. [34] analyzed invariance with respect to the benefits and limitations of data augmentation and feature averaging, presenting both theoretical and empirical arguments for using feature averaging over data augmentation. More recently, Chen et al. [6] presented a useful group-theoretic framework with which to understand data augmentation. Relevant to the present work, Chen et al. [5] introduced a notion of *approximate invariance*. Unlike that work, however, which focused on theoretical results related to data augmentation, this paper aims to introduce metrics that can be applied to modern deep learning architectures and answers questions about invariance from an empirical perspective. There are a number of existing works that proposed metrics aimed at measuring the extent to which a model is not equivariant (e.g. [8; 22; 18; 43; 49]). Our work differs from these in two ways: (1) we build general metrics based on basic group theory that are designed to work across different groups and datatypes and (2) unlike other works that use their metric to evaluate the equivariance of a specific model, we use our metrics to explore how models learn (or do not learn) to be equivariant generally.

Finally, a range of recent works have shown that even beyond the standard evaluation statistics (e.g., accuracy), invariance is an important concept to consider when studying deep learning models. For example, Kaur et al. [25] showed that lack of invariance can be used to identify out-of-distribution inputs. A further series of works investigated whether excessive invariance can reduce adversarial robustness [23; 24; 40]. All of this work reinforces one of the primary messages of this paper, that it is important to be able to measure invariance and equivariance directly in a model.

3 Quantifying Invariance and Equivariance

We begin this section by recalling the mathematical definitions of equivariance and invariance. We present these definitions in terms of the mathematical concept of a group, which formally captures the notion of symmetry [15].

Assume that G is a group. We say that G acts on sets X and Y if there are maps $\phi_X : G \times X \rightarrow X$ and $\phi_Y : G \times Y \rightarrow Y$ that respect the composition operation of G . That is, for $g_1, g_2 \in G$ and $x \in X$,

$$\phi_X(g_2, \phi_X(g_1, x)) = \phi_X(g_2 g_1, x),$$

with an analogous condition for ϕ_Y . Whenever the meaning is clear, we simplify notation by writing $\phi_X(g, x) = gx$ (with an analogous convention for ϕ_Y). A map $f : X \rightarrow Y$ is said to be G -equivariant if for all $x \in X$ and $g \in G$,

$$f(gx) = gf(x). \tag{1}$$

In the case where the map ϕ_Y is trivial so that $gy = y$ for all $g \in G$ and $y \in Y$, we say that f is G -invariant. Thus, invariance is a special case of equivariance.

Assume that $f : X \rightarrow Y$ is a neural network where X is the ambient space of input data and Y is the target space. In many cases there is a natural way to factorize f into a composition $f = f_2 \circ f_1$ where $f_1 : X \rightarrow Z$ is known as the feature extractor, Z is the latent space of f , and $f_2 : Z \rightarrow Y$ is the classifier. For example, if f is a ResNet50 CNN [20] then f_1 may consist of all residual blocks while f_2 would consist of the final affine classification and softmax layers. We say that machine learning model f extracts G -equivariant features if f_1 is a G -equivariant function. This is an especially meaningful distinction in the context of transfer learning where invariance or equivariance can be transferred to a new task via the invariance or equivariance of f_1 . Note that the definition of G -equivariant feature extraction requires a well-defined action of G on Z , which may not be obvious in many cases. Because the trivial action is defined for any G and Z , we can always ask whether f extracts G -invariant features.

The following proposition provides some insight into how the invariance (or lack of invariance) of f_1 relates to the invariance (or lack of invariance) of f .

Proposition 3.1. Let $f : X \rightarrow Y$ be a function that decomposes into $f = f_2 \circ f_1$ where $f_1 : X \rightarrow Z$ and $f_2 : Z \rightarrow Y$. Suppose that G acts on $X, Z,$ and Y .

1. f can be G -invariant even if f_1 and f_2 are not.
2. If f_1 is G -invariant, then f is G -invariant.

A proof of Proposition 3.1 can be found in Section A.5. Note that Proposition 3.1.2 implies that if earlier layers of a network achieve invariance with respect to some group, then this invariance will persist into later layers. This may be seen as part of the justification of the common practice within the equivariant architectures community of building invariance through successive combinations of G -equivariant layers and pooling layers. Of course, the statement holds only when exact invariance is achieved. We see below that this is not generally the case.

3.1 Measuring equivariance

In this section we assume that both X and Y are vector spaces and the action of G on both X and Y is linear. In all of our experiments we assume that the action of G on X and Y is known. In the case that f is also a linear map, the equivariance of f can be checked directly by checking equivariance on a basis for X . By extension, the equivariance of many common types of neural network layers can be checked when these can be framed as linear maps (e.g., convolutional layers). However, there is no systematic procedure for checking the equivariance of a nonlinear function f . If f is the composition of a sequence of functions f_1, f_2, \dots, f_n and we can check that each is equivariant, then we know that f is equivariant, but we cannot prove that a function is not equivariant just by proving that each layer is not equivariant (this follows from Proposition 3.1.1). We are thus motivated to introduce a family of metrics that can be used to empirically measure the extent to which a function deviates from being equivariant on a data distribution \mathcal{D} on X .

Since we assume in this section that the action of G on Y is linear, we can define the kernel of this action, $\ker(\phi_Y)$, which is a subgroup of G . $\ker(\phi_Y)$ consists of all those $g \in G$ such that g acts as the identity on Y . For $x \in X$, we define $\hat{f}(x)$ to be the expected value of $f(gx)$ over $\ker(\phi_Y)$,

$$\hat{f}(x) := \mathbb{E}_{g \in \ker(\phi_Y)}(f(gx)) = \int_{g \in \ker(\phi_Y)} f(gx) d\mu \quad (2)$$

where μ is the usual normalized Haar measure on subgroup $\ker(G)$. Note that when f is G -equivariant, then for each $g \in \ker(\phi_Y)$, $f(gx) = gf(x) = f(x)$ and hence $\hat{f} = f$.

Let (\mathcal{D}, ν) be a probability distribution on X and let $m : Y \times Y \rightarrow \mathbb{R}_{\geq 0}$ be a distance function on Y . We can use m to measure the extent to which f deviates from being G -equivariant by computing

$$\int_{\mathcal{D}} \int_{g \in G} m(f(gx), g\hat{f}(x)) d\mu dx \quad (3)$$

where this time μ is the normalized Haar measure on G . Note that the argument $m(f(gx), g\hat{f}(x))$ measures the extent to which (1) fails to hold across distribution \mathcal{D} , except that $gf(x)$ is replaced by $g\hat{f}(x)$. We use $\hat{f}(x)$ because it averages over all values in the orbit of x (under G) that should map to $f(x)$. If f were genuinely G -equivariant, all these values $f(gx)$ would yield $f(x)$. This choice is supported by the fact that it naturally interpolates between the two extreme cases: G acts trivially on Y (invariance) and G acts faithfully on Y . In the former case $\hat{f}(x)$ is the average value of $f(gx)$ over all of $g \in G$ and in the latter case $\hat{f}(x) = f(x)$.

The proposition below proves that when the action of G is faithful on X, Y , (3) being 0 is equivalent to f satisfying (1) on a set of measure 1.

Proposition 3.2. Let $f : X \rightarrow Y$ be a continuous function, G a group that acts linearly and faithfully on both X and Y , and $m : Y \times Y \rightarrow \mathbb{R}_{\geq 0}$ a metric. Let \mathcal{D} be a distribution on X . Then (3) is zero if and only if f is G -equivariant almost surely, i.e., on a set of measure 1.

We provide a proof of Proposition 3.2 in Appendix A.6

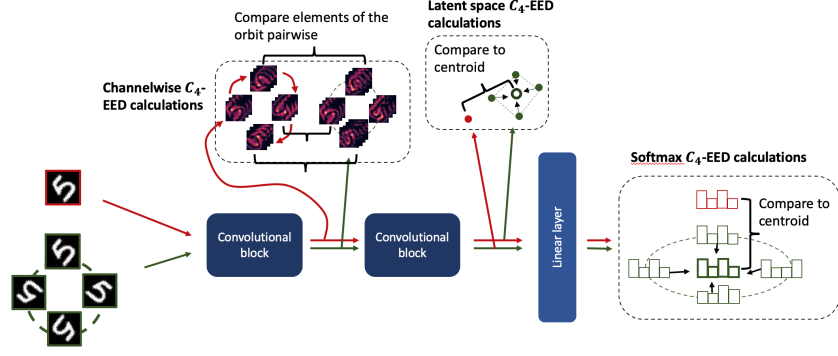


Figure 1: A diagram illustrating the different types of empirical equivariance deviation (EED) that we investigate in this paper for the rotation action of cyclic group C_4 on MNIST images.

To approximate (3) for real models and data where we always work with finite groups and finite samples of \mathcal{D} , we define the G -EED of f with respect to m to be

$$\mathcal{E}(f, G) := \frac{1}{|\mathcal{D}||G|} \sum_{x \in \mathcal{D}} \sum_{g \in G} m(f(gx), g\hat{f}(x)). \quad (4)$$

Note that since G is a finite group (and hence discrete), the Haar measure turns into the usual counting measure.

In the remainder of this section we describe some specific types of G -EED that may be relevant to computer vision tasks. By convention, when using a distance function m for which larger values of $m(x_1, x_2)$ indicates that x_1 and x_2 are “closer” (the opposite of a proper metric), we attach a negative sign to m . For example, rather than using cosine similarity, we use negative cosine similarity (e.g., (5)). This way, larger values of G -EED consistently indicate less invariance, regardless of the m used.

The channelwise G -equivariance of convolutional layer activations: Throughout most layers of a CNN an individual image is represented as a 3-tensor. Let $f_\ell : X \rightarrow \mathbb{R}^{C_\ell \times H_\ell \times W_\ell}$ be the composition of the first ℓ layers of a CNN such that for input image $x \in X$, $f_\ell(x)$ is a $C_\ell \times H_\ell \times W_\ell$ tensor where the first dimension corresponds to the channels of the representation and the second and third dimensions correspond to the two spatial dimensions.

Suppose that G is a finite group that acts on images and other 2-tensors (e.g., rotations, translations, and reflections). To understand the extent to which the first ℓ layers of the network are G -equivariant, we can measure the G -EED of f_ℓ . Although there are numerous choices of m for (3) that could be used to measure the channelwise difference between $f_\ell(gx)$ and $g\hat{f}_\ell(x)$, we choose the following: let $S : \mathbb{R}^{H_\ell \times W_\ell} \times \mathbb{R}^{H_\ell \times W_\ell} \rightarrow [0, 1]$ be the cosine similarity on individual channels treated as vectors in $\mathbb{R}^{H_\ell W_\ell}$. Write $[f_\ell(x)]_i$ for the i th channel of $f_\ell(x)$. Then we set

$$m(f_\ell(gx), g\hat{f}_\ell(x)) = -\frac{1}{C} \sum_{i=1}^C S([f_\ell(gx)]_i, g[\hat{f}_\ell(x)]_i).$$

That is, let m be the negative of the average cosine similarity between individual channels of $f_\ell(gx)$ and $g\hat{f}_\ell(x)$. This gives:

$$\mathcal{E}_{\text{channel}}(f, G, \ell) := \frac{1}{|\mathcal{D}||G|} \sum_{x \in \mathcal{D}} \sum_{g \in G} m(f_\ell(gx), g\hat{f}_\ell(x)) \quad (5)$$

Note that since rotation, translation, and reflection groups all act faithfully on $\mathbb{R}^{H_\ell \times W_\ell}$, for these specific G , $\hat{f} = f$. We call this version of G -EED *channelwise G -EED*. This metric assumes that G acts on each channel in a 3-tensor independently. It does not account for the more complicated setting where the action of G either permutes or mixes channels of $\mathbb{R}^{C_\ell \times H_\ell \times W_\ell}$ in a non-trivial way. In this work we always assume that the action of G on channels of $\mathbb{R}^{C_\ell \times H_\ell \times W_\ell}$ is identical to the action of G on X (up to differences in spatial scale and number of channels). We consider the case where

the action of G on $\mathbb{R}^{C_\ell \times H_\ell \times W_\ell}$ may permute channels in $\mathbb{R}^{C_\ell \times H_\ell \times W_\ell}$ in Appendix A.4. But here, if $G = C_8$ and G rotates the spatial dimension of input images, we assume G rotates each individual channel of hidden representations as well.

Invariance of latent space representations: Consider a model f consisting of feature extractor $f_1 : X \rightarrow \mathbb{R}^k$ and classifier $f_2 : \mathbb{R}^k \rightarrow \mathbb{R}^n$. If G is some group that acts on X , we can ask whether f_1 extracts G -invariant features. Define M to be either the average ℓ_2 -distance or cosine similarity between distinct points in the set $f_1(D)$. By setting m to be the ℓ_2 -distance (respectively cosine similarity), we calculate the *latent space G -EED* as

$$\mathcal{E}_{\text{latent}}(f, G) := \frac{1}{M} \frac{1}{|D||G|} \sum_{x \in D} \sum_{g \in G} m(f_1(gx), \hat{f}_1(x)). \quad (6)$$

Note that because in this setting G acts trivially on the latent space \mathbb{R}^k (because of the invariance assumption), $\hat{f}_1(x) = \frac{1}{|G|} \sum_{g \in G} f_1(gx)$. We describe why the normalization term M is necessary in Section A.7 of the Appendix. See also Figure 14. As we show in Section 4.1, it is often useful to consider latent space G -EED with respect to both Euclidean distance and negative cosine similarity.

Invariance at the softmax layer of classifiers:

While the two examples above focused on calculating invariance and equivariance at different intermediate layers of computer vision models, invariance of classification models is most commonly considered with respect to the final softmax output. In this paper we choose to use KL-divergence for m because it is a distance function designed to handle probability distributions, which softmax outputs approximate. In particular,

$$\mathcal{E}_{\text{softmax}}(f, G) := \frac{1}{|D||G|} \sum_{x \in D} \sum_{g \in G} D_{KL}(f(gx), \hat{f}(x)).$$

We call this metric the *softmax G -EED*.

4 Understanding invariance and equivariance in deep learning

To prototype G -EED we experiment with the finite cyclic group C_8 that acts on images by 45° rotations. This symmetry is relevant to datasets where imagery does not have a preferred orientation. The datasets we use include *Rotated MNIST* which consists of randomly rotated MNIST digits [14] from classes 0-8 and *xView Maritime*, a chipped version of the xView object detector overhead dataset [31] composed of the nine maritime classes. We chose xView Maritime because it is a more real-world dataset that has an obvious symmetry (rotation) that is not hardcoded into standard CNNs. We describe these and other datasets we use in detail in Section A.2.

To reduce the computational burden, when calculating (4) we only used 50 randomly chosen examples from the corresponding dataset. We found that evaluating at more points did not substantially change the results. When not otherwise stated all invariance and equivariance measurements were calculated using points from the test set, not the training set. The normalization constant for latent space G -EED is calculated over 200 randomly chosen points.

4.1 Do networks trained with augmentation learn equivariant layers?

In this section we apply our metrics to standard CNNs and C_8 -rotation equivariant, steerable CNNs (C_8 -CNN) [45] to compare the invariance or equivariance of a model trained with augmentation with the invariance or equivariance of a model that is explicitly designed to learn invariance through progressive equivariant layers and pooling. We train 10 copies of each model type for 2,000 iterations on rotated MNIST. We apply random rotation augmentation to the models during training and all achieve an accuracy of over 98% on the test set. By design, for any $1 \leq k \leq 6$, the first k -blocks of one of the C_8 -CNN models will be approximately rotation equivariant (up to hardcoded permutation of channels which we take into consideration when applying our metrics). The standard wisdom is that, with pooling, this will lead to an invariant representation in the latent space.

Despite the fact that both families of models achieve similar performance, we note that their invariance and equivariance properties differ significantly. The channelwise C_8 -EED of the composition of

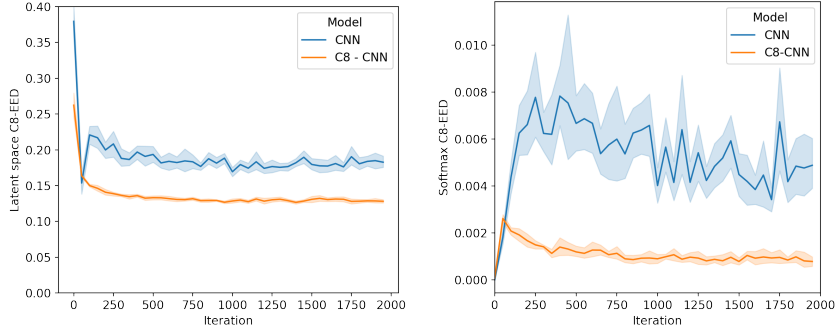


Figure 2: The latent space C_8 -EED (left) and softmax C_8 -EED (right) for conventional and C_8 -equivariant CNNs (C_8 -CNNs) [45] with respect to the rotated MNIST dataset. Both plots include 95% confidence intervals. Lower values for both plots indicate more C_8 -invariance. 95% confidence intervals are over 10 randomly initialized models.

the first k blocks (where $1 \leq k \leq 6$) of the C_8 -CNN is significantly higher than that of the CNN, indicating that (as claimed) the C_8 -CNN is more equivariant with respect to individual channel rotations of 45° in both input and hidden representations (see Figure 7). Beyond that we see that equivariance decays for both models as input travels through additional blocks. This is particularly true for the C_8 -CNN. We conjecture that this is likely caused by the accumulation of interpolation artifacts associated with rotation. Perhaps even more interesting is the fact that for no layer of either model do the channelwise C_8 -EED values increase beyond a small jump at the beginning of training. This suggests that layerwise equivariance may not always be aligned with the learning objective and that learned invariance does not arise through the naive form of learned equivariance.

Both in terms of the Euclidean distance version of latent space C_8 -EED and softmax C_8 -EED, the C_8 -CNNs show more invariance than the conventional CNNs (see Figure 2) but the difference is less dramatic than it is for channelwise C_8 -EED. This suggests that the CNNs likely catch up in terms of C_8 -invariance using mechanisms distinct from layerwise C_8 -equivariance. Notable also is the fact that unlike channelwise C_8 -EED, which did not indicate increased C_8 -equivariance over the course of training, both latent space and softmax C_8 -EED decreased with training (suggesting learned invariance at these layers).

Most surprisingly, in Figure 8 (left) we see that the C_8 -CNNs are less invariant than the conventional CNNs with respect to the cosine similarity version of latent space C_8 -EED. We conjecture two possible reasons for this. The first is based on the fact that C_8 -CNNs are designed to be equivariant **on the nose, not up to scaling**. The structural constraint of exact equivariance may actually be misaligned with cosine similarity where vector magnitude no longer matters. From this perspective, projective representation theory, where symmetries are only taken up to scaling, might be a profitable direction of future research in equivariant architectures. The second possible explanation arises from Figure 8 (right) which shows that in terms of absolute cosine similarity (that is, without the normalization term M in (6)), the C_8 -CNN is more invariant. It may be that while C_8 -CNNs indeed cluster orbits of points under the C_8 action closer together, the conventional CNNs are better at spreading other points further away in the latent space.

Summary: Equivariant architectures and nonequivariant architectures capture invariance in distinct ways. Nonequivariant networks do not learn layerwise equivariance (at least with respect to the naive C_8 action given by rotating individual channels in a hidden representation). Rather, their invariance seems to be captured by the final layers. The level of invariance measured in the latent space depends on the underlying metric m which is used.

4.2 Does learned invariance hold for out-of-distribution data?

It was noted in Lyle et al. [34] that while augmentation may be satisfactory for many tasks, there is a risk that learned invariance will not extend to out-of-distribution (OOD) data. We investigate this question using G -EED metrics, studying the conventional CNN and C_8 -equivariant CNN from

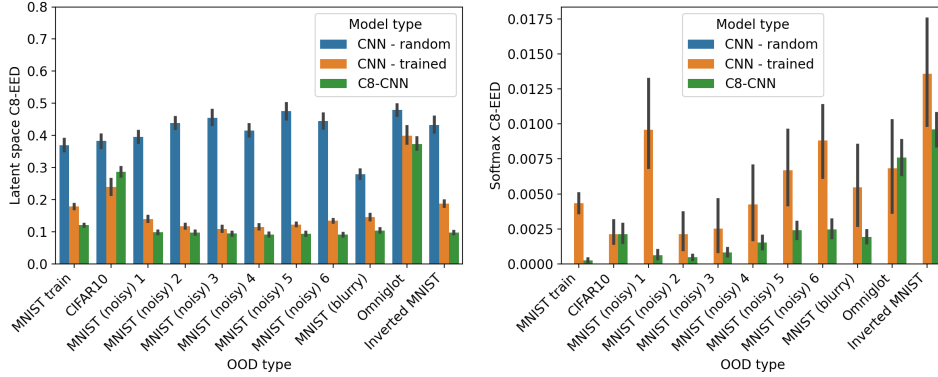


Figure 3: The latent space C_8 -EED (left) and softmax C_8 -EED (right) for conventional untrained CNNs, conventional CNNs trained on MNIST, and C_8 -equivariant CNNs (C_8 -CNNs) [45] trained on MNIST with respect to a range of in- and out-of-distribution datasets. Both plots include 95% confidence intervals over 10 randomly initialized models.

Section 4.1 and a conventional CNN with untrained weights that can be used for comparison. Note that because rotation invariance is at some level hardcoded into the architecture of the C_8 -CNN, our default assumption is that the C_8 -CNN models will tend to be more invariant on OOD data than models with learned augmentation. Images of example OOD data as well as dataset descriptions can be found in Appendix A.2.

The left plot in Figure 3 shows the latent space C_8 -EED for the three model families that we tested. We can see that random weights extract significantly less invariant latent space representations compared to both the augmentation-trained CNNs and C_8 -CNNs. Although this difference is not surprising for the C_8 -CNNs, for the standard CNNs it indicates that augmentation does learn some rotation-invariant features that generalize to OOD data. Furthermore, while C_8 -CNNs do exhibit more latent space invariance than the augmentation-trained CNNs, the difference is insignificant compared to the difference between augmentation-trained CNNs and CNNs with random weights. Note that in these OOD experiments, the normalization term M in (6) is calculated using the OOD data (rather than the training or test set). This choice was made when considering situations in which a frozen network is used in combination with metric learning methods, as in Snell et al. [42], to solve a task with data drawn from a shifted distribution.

As a showcase of how a single model can display different types of invariance, the CNNs with random weights are far more invariant in terms of softmax C_8 -EED than the trained C_8 -CNN, which is more invariant than the trained CNN (right plot, Figure 3). We suspect that invariance of the CNNs with random weights arises from the fact that an untrained network tends to be insensitive to input. This observation is useful to keep in mind, especially as the concept of invariance is frequently treated as a net benefit to any model. Invariance is useful when it is aligned with other metrics more directly related to the task the model was designed for.

Summary: Our experiments suggest that augmentation trained networks do learn invariance that mildly generalizes to OOD data. A single model can display differing kinds of invariance (an untrained network does not extract invariant features but through insensitivity may make invariant predictions). In cases where invariance is critical and OOD data is expected, equivariant architectures may be a safer choice than training with augmentation.

4.3 How does the use of pretrained weights affect invariance and equivariance?

It has become standard practice in computer vision to initialize a model using weights trained on a large, diverse image dataset such as ImageNet [13]. It is reasonable to ask how such a strategy affects the invariance and equivariance of the resulting models. We choose four different image classifier architectures: ResNet50 [20], AlexNet [29], DenseNet121 [21], and LeViT192 [1]. For each of these architectures, we initialized five models with random weights and five models with weights from either the Torchvision package [35] (ResNet50, AlexNet, and DenseNet) or Timm [48] (LeViT192).

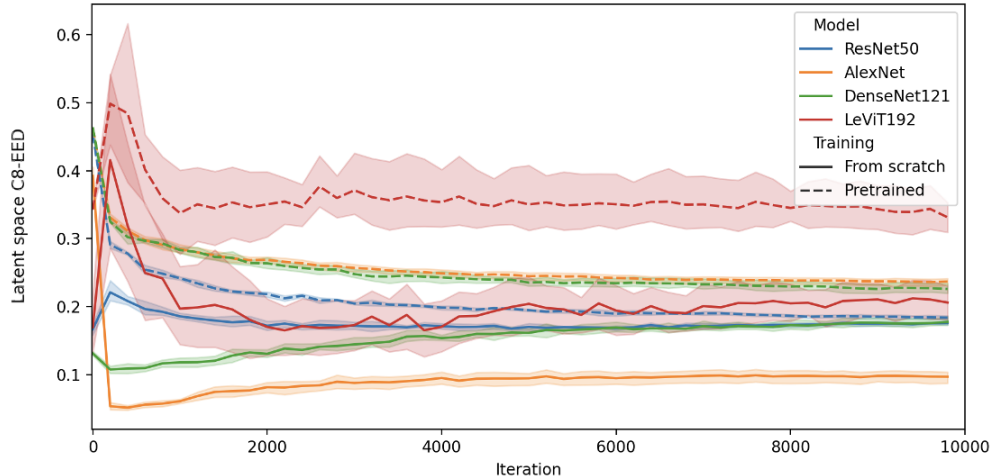


Figure 4: The latent space C_8 -EED measured every 200 training iterations (for a total of 10,000 iterations) for a range of model architectures that were initialized with either random or ImageNet pretrained weights. Confidence intervals are over 5 randomly initialized models for ‘from scratch’ and 5 independent trainings for ‘pretrained’.

We then trained all of these models on the xView Maritime training set. Next, we evaluated the latent space C_8 -EED and softmax C_8 -EED on the xView Maritime test set. It is important to note that pretrained weights, which were generated by training on ImageNet, might not be expected to have learned to extract fully rotationally invariant features. Indeed, the objects found in ImageNet mostly have a preferred orientation at which they generally are seen (there are very few instances of upside-down dogs or vehicles in ImageNet).

Figure 4 shows the latent space C_8 -EED for all eight model types recorded every 200 iterations. We see that in this experiment and for this specific metric, models trained from scratch extract more invariant features in their latent space. Moreover, while the invariance of models trained from scratch tends to decrease slightly over the course of training (latent space C_8 -EED increases), the invariance of models trained using pretrained weights tends to increase slightly. This may relate to ImageNet’s lack of object classes that appear at a wide range of orientations. The models with pretrained weights may need to learn additional rotation invariance. Contrast that with the weights trained from scratch that may learn non-robust rotation invariant features early which are refined to less rotationally invariant features that better optimize the cross-entropy loss function later. This, along with the fact that models using pretrained weights tend to have slightly higher accuracy, points to a complicated dynamics between model robustness, model invariance, and model performance which likely requires further exploration. We also calculated the latent space D_8 -EED (where D_8 is the order 16 dihedral group) for these same models and dataset. The results are recorded in Figure 10. We find the patterns to be fairly similar.

On the other hand, Figure 16 in the Appendix shows that, in terms of C_8 -EED, the invariance properties of pretrained networks vs. networks trained from scratch is somewhat more ambiguous.

Summary: Our experiments make it clear that the extent to which invariances are learned differs between networks using pretrained weights and networks trained from scratch.

4.4 The invariance of supervised and self-supervised models

In an additional experiment, we compared the invariance of supervised models to the invariance of self-supervised models. To do this we evaluated four different convolutional neural networks in one of the simplest possible settings where G is the order 2 group of reflections across the vertical axis. The models we chose to test were a standard ResNet50 (we used the Torchvision pretrained weights) [20; 35], a Big Transfer ResNet50V2_101 [26] (with weights from ‘PyTorch Image Models’ [48]), a ResNet50 trained using the self-supervised method DINO (we used the author’s pretrained weights)

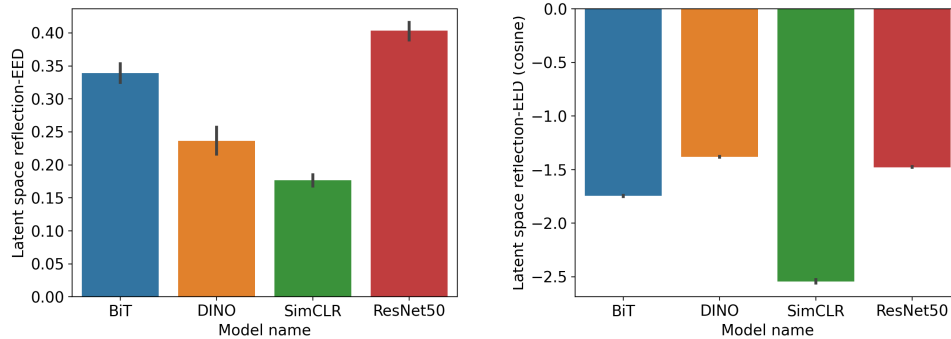


Figure 5: Latent space G -EED for two models trained using supervised methods (BiT and ResNet50) and two models trained using self-supervised methods (DINO and SimCLR), where G is the order 2 group of reflections across the vertical axis. SimCLR is the only model trained with contrastive loss. All models use some version of the ResNet architecture. **(Left)** The standard latent space G -EED metric. **(Right)** G -EED where cosine similarity is used instead of Euclidean distance. Error bars represent 95% confidence intervals over 100 random inputs from the ImageNet test set.

[4], and a ResNet50 trained using the self-supervised method SimCLR [7] (we used weights from [44]). Note that the first two models utilized supervised training (with different size training sets) and the second two utilized self-supervised training techniques. Further, SimCLR is trained with a contrastive loss that directly optimizes for invariance of input to specific transformations (including reflection). On the other hand, DINO uses ‘knowledge distillation’, without a contrastive loss. We choose to concentrate on latent space G -EED in this experiment.

Our results can be found in Figure 5. Note that since all of these models have a 2048-dimensional latent space, we can directly compare them. This is something we could not do in Section 4.3. We see that in terms of both versions of latent space G -EED (that which uses Euclidean distance and that which uses cosine similarity), the model trained using SimCLR has significantly more invariance. This is not surprising given that the contrastive loss that SimCLR uses explicitly optimizes for similarity between an image and its reflection. DINO, which is also trained in a self-supervised manner, but which does not explicitly use the contrastive loss is less invariant (how it compares to the two supervised models depends on which metric is used).

Summary: Use of contrastive loss can improve invariance but otherwise there is not strong evidence that self-supervision increases model invariance.

5 Limitations and Conclusion

Although the G -EED family of metrics that we introduce is flexible in many ways, it is not capable of capturing notions of invariance that do not have a known underlying symmetry group (e.g., changes in image background), do not come from the action of a group (e.g., scaling corresponding to a semigroup action), or (for the purpose of measuring equivariance of internal representations) do not have a known action on the hidden activations of a model (e.g., changes in color). An important next step would be to bring our metrics to these broader notions of invariance and equivariance. It would be particularly valuable if our metrics could be modified so that they can measure equivariance without explicitly specifying a group action in a hidden layer. This would enable us to measure G -EED for emergent types of learned equivariance where the action of G on the output space is not specified by the user.

In this paper we described a novel family of metrics meant to measure equivariance in deep learning models. We use these metrics to suggest answers to questions related to the extent to which neural networks are or are not invariant or equivariant to different types of transformations. Surprisingly, while invariance and equivariance are fundamental topics within machine learning, this is one of the first works (to our knowledge) that tries to broadly measure these properties empirically in modern

neural networks. We hope that this work will open a conversation on this important topic that will ultimately lead to a better understanding of why deep learning models behave the way that they do.

References

- [1] LeViT: a vision transformer in convnet’s clothing for faster inference. In *Proceedings of the IEEE/CVF International Conference on Computer Vision*, pages 12259–12269, 2021.
- [2] A. Antoniou, A. Storkey, and H. Edwards. Data augmentation generative adversarial networks. *arXiv preprint arXiv:1711.04340*, 2017.
- [3] B. Bloem-Reddy and Y. W. Teh. Probabilistic symmetries and invariant neural networks. *J. Mach. Learn. Res.*, 21:90–1, 2020.
- [4] M. Caron, H. Touvron, I. Misra, H. Jégou, J. Mairal, P. Bojanowski, and A. Joulin. Emerging properties in self-supervised vision transformers. In *Proceedings of the International Conference on Computer Vision (ICCV)*, 2021.
- [5] S. Chen, E. Dobriban, and J. H. Lee. Invariance reduces variance: Understanding data augmentation in deep learning and beyond. 2019.
- [6] S. Chen, E. Dobriban, and J. Lee. A group-theoretic framework for data augmentation. *Advances in Neural Information Processing Systems*, 33:21321–21333, 2020.
- [7] T. Chen, S. Kornblith, M. Norouzi, and G. Hinton. A simple framework for contrastive learning of visual representations. In *International conference on machine learning*, pages 1597–1607. PMLR, 2020.
- [8] O. J. Cobb, C. G. Wallis, A. N. Mavor-Parker, A. Marignier, M. A. Price, M. d’Avezac, and J. D. McEwen. Efficient generalized spherical CNNs. *arXiv preprint arXiv:2010.11661*, 2020.
- [9] T. Cohen and M. Welling. Group equivariant convolutional networks. In *International conference on machine learning*, pages 2990–2999. PMLR, 2016.
- [10] T. S. Cohen and M. Welling. Steerable CNNs. *arXiv preprint arXiv:1612.08498*, 2016.
- [11] T. S. Cohen, M. Geiger, J. Köhler, and M. Welling. Spherical CNNs. *arXiv preprint arXiv:1801.10130*, 2018.
- [12] E. D. Cubuk, B. Zoph, D. Mane, V. Vasudevan, and Q. V. Le. Autoaugment: Learning augmentation policies from data. *arXiv preprint arXiv:1805.09501*, 2018.
- [13] J. Deng, W. Dong, R. Socher, L.-J. Li, K. Li, and L. Fei-Fei. ImageNet: A Large-Scale Hierarchical Image Database. In *CVPR09*, 2009.
- [14] L. Deng. The MNIST database of handwritten digit images for machine learning research. *IEEE Signal Processing Magazine*, 29(6):141–142, 2012.
- [15] D. S. Dummit and R. M. Foote. *Abstract algebra*, volume 3. Wiley Hoboken, 2004.
- [16] C. Esteves, C. Allen-Blanchette, A. Makadia, and K. Daniilidis. Learning SO(3) equivariant representations with spherical CNNs. In *Proceedings of the European Conference on Computer Vision (ECCV)*, pages 52–68, 2018.
- [17] G. B. Folland. *Real analysis: modern techniques and their applications*, volume 40. John Wiley & Sons, 1999.
- [18] F. Fuchs, D. Worrall, V. Fischer, and M. Welling. SE(3)-transformers: 3D roto-translation equivariant attention networks. *Advances in Neural Information Processing Systems*, 33:1970–1981, 2020.
- [19] S. Hauberg, O. Freifeld, A. B. L. Larsen, J. Fisher, and L. Hansen. Dreaming more data: Class-dependent distributions over diffeomorphisms for learned data augmentation. In *Artificial Intelligence and Statistics*, pages 342–350. PMLR, 2016.

- [20] K. He, X. Zhang, S. Ren, and J. Sun. Deep residual learning for image recognition. In *Proceedings of the IEEE conference on computer vision and pattern recognition*, pages 770–778, 2016.
- [21] G. Huang, Z. Liu, L. Van Der Maaten, and K. Q. Weinberger. Densely connected convolutional networks. In *Proceedings of the IEEE conference on computer vision and pattern recognition*, pages 4700–4708, 2017.
- [22] M. J. Hutchinson, C. Le Lan, S. Zaidi, E. Dupont, Y. W. Teh, and H. Kim. Lietransformer: Equivariant self-attention for Lie groups. In *International Conference on Machine Learning*, pages 4533–4543. PMLR, 2021.
- [23] J.-H. Jacobsen, J. Behrmann, R. Zemel, and M. Bethge. Excessive invariance causes adversarial vulnerability. *arXiv preprint arXiv:1811.00401*, 2018.
- [24] S. Kamath, A. Deshpande, and K. Subrahmanyam. Invariance vs robustness of neural networks. 2019.
- [25] R. Kaur, S. Jha, A. Roy, S. Park, E. Dobriban, O. Sokolsky, and I. Lee. idecode: In-distribution equivariance for conformal out-of-distribution detection, 2022.
- [26] A. Kolesnikov, L. Beyer, X. Zhai, J. Puigcerver, J. Yung, S. Gelly, and N. Houlsby. Big transfer (BiT): General visual representation learning. In *European conference on computer vision*, pages 491–507. Springer, 2020.
- [27] R. Kondor and S. Trivedi. On the generalization of equivariance and convolution in neural networks to the action of compact groups. In *International Conference on Machine Learning*, pages 2747–2755. PMLR, 2018.
- [28] A. Krizhevsky, G. Hinton, et al. Learning multiple layers of features from tiny images. 2009.
- [29] A. Krizhevsky, I. Sutskever, and G. E. Hinton. Imagenet classification with deep convolutional neural networks. In *Proceedings of the 25th International Conference on Neural Information Processing Systems - Volume 1, NIPS’12*, page 1097–1105, Red Hook, NY, USA, 2012. Curran Associates Inc.
- [30] B. M. Lake, R. Salakhutdinov, and J. B. Tenenbaum. Human-level concept learning through probabilistic program induction. *Science*, 350(6266):1332–1338, 2015.
- [31] D. Lam, R. Kuzma, K. McGee, S. Dooley, M. Laielli, M. Klaric, Y. Bulatov, and B. McCord. xView: Objects in context in overhead imagery. *arXiv preprint arXiv:1802.07856*, 2018.
- [32] Y. LeCun, P. Haffner, L. Bottou, and Y. Bengio. Object recognition with gradient-based learning. In *Shape, contour and grouping in computer vision*, pages 319–345. Springer, 1999.
- [33] J. Lee, Y. Lee, J. Kim, A. Kosiorek, S. Choi, and Y. W. Teh. Set transformer: A framework for attention-based permutation-invariant neural networks. In K. Chaudhuri and R. Salakhutdinov, editors, *Proceedings of the 36th International Conference on Machine Learning*, volume 97 of *Proceedings of Machine Learning Research*, pages 3744–3753. PMLR, 09–15 Jun 2019. URL <https://proceedings.mlr.press/v97/lee19d.html>.
- [34] C. Lyle, M. van der Wilk, M. Kwiatkowska, Y. Gal, and B. Bloem-Reddy. On the benefits of invariance in neural networks. *arXiv preprint arXiv:2005.00178*, 2020.
- [35] S. Marcel and Y. Rodriguez. Torchvision the machine-vision package of torch. In *Proceedings of the 18th ACM international conference on Multimedia*, pages 1485–1488, 2010.
- [36] D. Marcos, M. Volpi, N. Komodakis, and D. Tuia. Rotation equivariant vector field networks. In *Proceedings of the IEEE International Conference on Computer Vision*, pages 5048–5057, 2017.
- [37] A. J. Ratner, H. Ehrenberg, Z. Hussain, J. Dunnmon, and C. Ré. Learning to compose domain-specific transformations for data augmentation. *Advances in neural information processing systems*, 30, 2017.

- [38] L. Sifre and S. Mallat. Combined scattering for rotation invariant texture analysis. In *ESANN*, volume 44, pages 68–81. Citeseer, 2012.
- [39] L. Sifre and S. Mallat. Rotation, scaling and deformation invariant scattering for texture discrimination. In *Proceedings of the IEEE conference on computer vision and pattern recognition*, pages 1233–1240, 2013.
- [40] V. Singla, S. Ge, B. Ronen, and D. Jacobs. Shift invariance can reduce adversarial robustness. *Advances in Neural Information Processing Systems*, 34, 2021.
- [41] L. Sixt, B. Wild, and T. Landgraf. Rendergan: Generating realistic labeled data. *Frontiers in Robotics and AI*, 5:66, 2018.
- [42] J. Snell, K. Swersky, and R. Zemel. Prototypical networks for few-shot learning. *Advances in neural information processing systems*, 30, 2017.
- [43] I. Sosnovik, M. Szmaja, and A. Smeulders. Scale-equivariant steerable networks. *arXiv preprint arXiv:1910.11093*, 2019.
- [44] J. Spijkervet. Simclr. <https://github.com/Spijkervet/SimCLR>, 2020.
- [45] M. Weiler and G. Cesa. General $E(2)$ -equivariant steerable CNNs. *Advances in Neural Information Processing Systems*, 32:14334–14345, 2019.
- [46] M. Weiler, M. Geiger, M. Welling, W. Boomsma, and T. Cohen. 3D steerable CNNs: Learning rotationally equivariant features in volumetric data.
- [47] M. Weiler, F. A. Hamprecht, and M. Storath. Learning steerable filters for rotation equivariant CNNs. In *Proceedings of the IEEE Conference on Computer Vision and Pattern Recognition*, pages 849–858, 2018.
- [48] R. Wightman. Pytorch image models. <https://github.com/rwightman/pytorch-image-models>, 2019.
- [49] D. Worrall and M. Welling. Deep scale-spaces: Equivariance over scale. *Advances in Neural Information Processing Systems*, 32, 2019.
- [50] D. E. Worrall, S. J. Garbin, D. Turmukhambetov, and G. J. Brostow. Harmonic networks: Deep translation and rotation equivariance. In *Proceedings of the IEEE Conference on Computer Vision and Pattern Recognition*, pages 5028–5037, 2017.
- [51] K. Xiao, L. Engstrom, A. Ilyas, and A. Madry. Noise or signal: The role of image backgrounds in object recognition. *arXiv preprint arXiv:2006.09994*, 2020.
- [52] R. Zhang. Making convolutional networks shift-invariant again. In *International conference on machine learning*, pages 7324–7334. PMLR, 2019.

A Appendix

A.1 Experimental Details

All our models were trained on an Nvidia A100 using the Adam optimizer. Batch size, learning rate (LR), and weight decay hyperparameters are summarized in the table below. Recall from Sections 4.1 through 4.3 that we train the CNNs and C_8 -CNNs (architecture description below) on rotated MNIST and train AlexNet, ResNet50, DenseNet121, and LeViT192 on Maritime xView. Hyperparameters were chosen based on an informal search. Running our experiments with a more comprehensive hyperparameter search would be a worthwhile future exercise since it might yield insight into how different hyperparameters affect model invariance and equivariance.

The standard CNN and C_8 -CNN used in Section 4.1 consist of 6 convolutional blocks, each containing a standard convolutional layer, a batch norm, a ReLU nonlinearity, and a pooling layer. The C_8 -CNN models have an analogous 6 block structure with the difference that each block uses C_8 -rotation equivariant, steerable convolutional layers and a so-called inner batch norm (a batch norm adapted for equivariant frameworks [45]). Both model types have a final linear layer.

Table 1: Experimental hyperparameters.

	Batch size	LR	Weight Decay
CNN	64	5×10^{-4}	1×10^{-5}
C_8 -CNN	64	5×10^{-4}	1×10^{-5}
AlexNet	64	5×10^{-5}	1×10^{-5}
ResNet50	64	5×10^{-4}	1×10^{-5}
DenseNet121	64	1×10^{-5}	1×10^{-5}
LeViT192	64	5×10^{-5}	1×10^{-5}

A.2 Dataset Details

The datasets used in our experiments include (i) *rotated MNIST*, which consists of images from MNIST rotated by random angles [14] (MNIST is covered by a Creative Commons Attribution-Share Alike 3.0 license) and (ii) *xView maritime*, a classification dataset we constructed by cropping the bounding boxes of all maritime vessel classes found in xView [31], an overhead imaging dataset (xView is covered by an Attribution-Noncommercial-ShareAlike 4.0 International (CC BY-NC-SA 4.0) license). In our version of rotated MNIST we excluded the class 9 so that we could remove the drop in model accuracy resulting from the similarity of a 9 and an upside-down 6. We apply a circular mask to all images before using them as input to a model so that invariance is not broken by the artifacts introduced by rotating a rectangular image by θ degrees where $\theta \neq 0^\circ, 90^\circ, 180^\circ, 270^\circ$. See the bottom right image in Figure 6 for an example of this.

Below we describe our OOD datasets for Section 4.2.

- **MNIST Train:** The original MNIST training images (with class 9 excluded).
- **CIFAR10:** Grayscale versions of the CIFAR10 images [28] (CIFAR10 is covered under an MIT license).
- **MNIST (Noisy) 1-6:** MNIST images perturbed by noise randomly sampled uniformly from intervals (1) $[0, 0.2]$, (2) $[0, 0.4]$, (3) $[0, 0.6]$, (4) $[0, 0.8]$, (5) $[0, 1.0]$, and (6) $[0, 1.2]$. Notice that any of these noise perturbations can push pixels outside of image bounds. We generally assume that images with more noise are farther OOD.
- **MNIST (blurry):** MNIST images with Gaussian blur applied with a size 7×7 kernel with standard deviation .5.
- **Omniglot:** Another image classification dataset that contains characters [30] (Omniglot is covered under an MIT license).
- **Inverted MNIST:** MNIST where each pixel has had the transformation $f(x) = 1 - x$ applied to it. This inverts the intensity of pixels to make the MNIST dataset look more like Omniglot (the background has high intensity and the digits have low intensity).

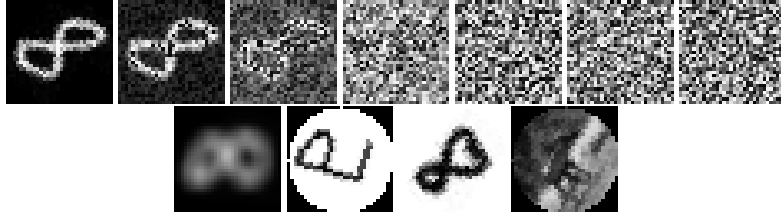


Figure 6: Examples of the OOD datasets that we used to evaluate our models. From left to right and top to bottom: MNIST train, MNIST (noisy) 1–6, MNIST (blurry), Omniglot, inverted MNIST, and CIFAR10 (grayscale).

A.3 How does invariance in a model’s latent space change when augmentation is or is not used?

As in Section 4.3, we focus on the case where $G = C_8$ (the group generated by 45° rotations) and the dataset xView Maritime. We trained 5 ResNet50s, 5 AlexNets, and 5 DenseNet121s with and without rotation augmentation respectively. We then measured latent space C_8 -EED in all models. Our results can be found in Figure 11. We find that models trained without augmentation indeed had consistently lower C_8 -EED both when we used our standard Euclidean distance metric and when we used the cosine similarity version. These experiments serve as evidence that our metrics are measuring the properties that we think they are measuring.

A.4 Does learned equivariance involve re-ordering of tensor channels?

Suppose that the function $f_\ell : X \rightarrow \mathbb{R}^{C_\ell \times H_\ell \times W_\ell}$ corresponds to the first ℓ layers of a network, terminating with a 3-tensor which has C_ℓ channels of height H_ℓ and width W_ℓ . Suppose that G is a group that acts both on the input space X and the hidden space $\mathbb{R}^{C_\ell \times H_\ell \times W_\ell}$. The channelwise G -EED metric that we proposed in this paper, assumes that when we compare channels from $f_\ell(gx)$ with channels from $gf_\ell(x)$, we should assume the trivial bijection. That is, we should compare the first channel of $f_\ell(gx)$, $[f_\ell(gx)]_1$, with the first channel of $gf_\ell(x)$, $[gf_\ell(x)]_1$, the second channel $[f_\ell(gx)]_2$ with the second channel $[gf_\ell(x)]_2$, etc.

On the other hand, in many equivariant CNN’s, the group action of g on $f_\ell(x)$ not only changes individual channels, it also permutes their order. It is reasonable to ask whether CNNs trained with augmentation might learn some similar “emergent” structure not only within individual channels, but also among them. The channelwise G -EED metric would likely not detect this kind of equivariance. In this section we examine this possibility. Though we do not disprove its existence, we run several preliminary experiments that suggest that this is not likely. This is an area that would benefit from additional study.

In our preliminary investigation, we focus on the filters at each layer (rather than input and output). We chose to do this based off of the observation that in equivariant CNNs that utilize the regular representation and which are designed to display the phenomenon we are looking for, filters come in entire orbits. That is, if w is a filter in a layer, then so is each element in the orbit Gw (i.e., the orbit of w under the action of G). In Figure 12 for example, four filters of a C_4 -equivariant convolutional layer [45] are displayed. The filters represent an orbit under the action of all 90-degree rotations (e.g., C_4).

As a first step towards identifying structured equivariance in augmentation trained CNNs, we compared all channels of each pair of filters at a given convolutional layer of an AlexNet CNN. However, comparing all the possible pairings is combinatorially prohibitive, even for simple architectures like AlexNet. In Figure 13, we plot the metric

$$\min_{\substack{j \neq i, k \\ g \in C_4}} \|g(w_{\ell, i, t}) - w_{\ell, j, k}\|_{\ell_2}, \quad (7)$$

where $w_{\ell, i, t}$ is the height H'_ℓ and weight W'_ℓ 2-tensor obtained by taking channel t from filter i in layer ℓ and $g(w_{\ell, i, t})$ is the action of group element g on $w_{\ell, i, t}$. It this case simply rotating by a multiple of 90° . We report the average of this metric over all convolutional layers of four different

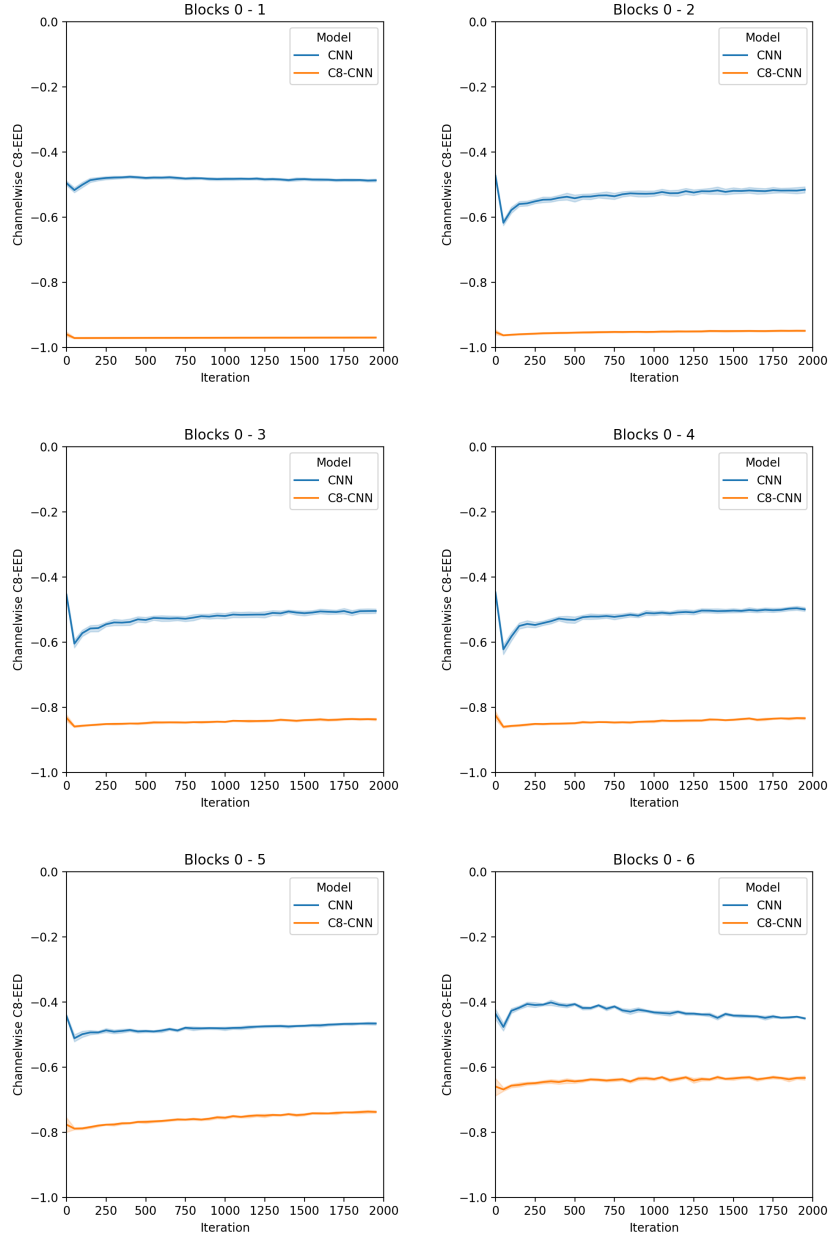


Figure 7: The channelwise C_8 -EED for the composition of various layers in 10 conventional CNNs and 10 C_8 -equivariant CNNs (C_8 -CNN) [45] trained on the rotated MNIST dataset. Both plots include 95% confidence intervals. Smaller values indicate more C_8 -equivariance.

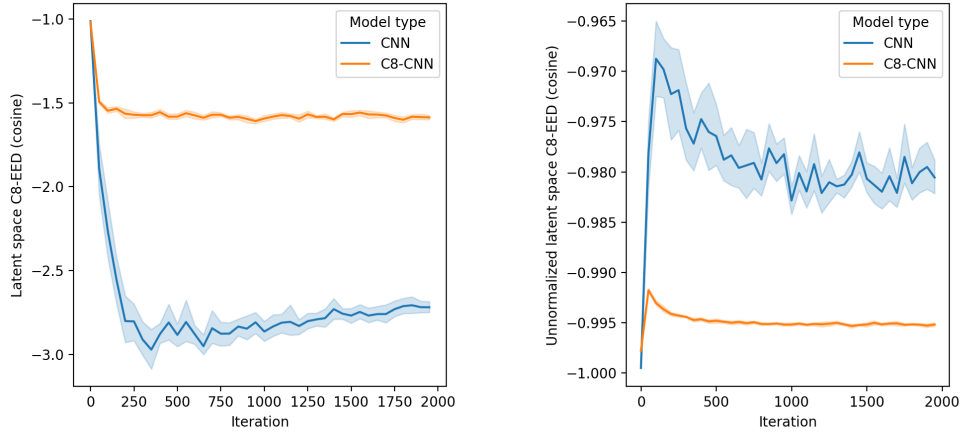


Figure 8: **(Left)** The cosine similarity version of latent space C_8 -EED for 10 conventional CNNs and 10 C_8 -CNNs all trained on rotated MNIST. Surprisingly, the C_8 -CNNs are **less** invariant with respect to this metric. We speculate as to why this might be in Section 4.1. **(Right)** One of our hypotheses is driven by plotting the unnormalized version of this metric which suggests that C_8 -CNNs clusters points in a single C_8 orbit closer than the CNNs, but do not scatter other points as far as the CNNs do.

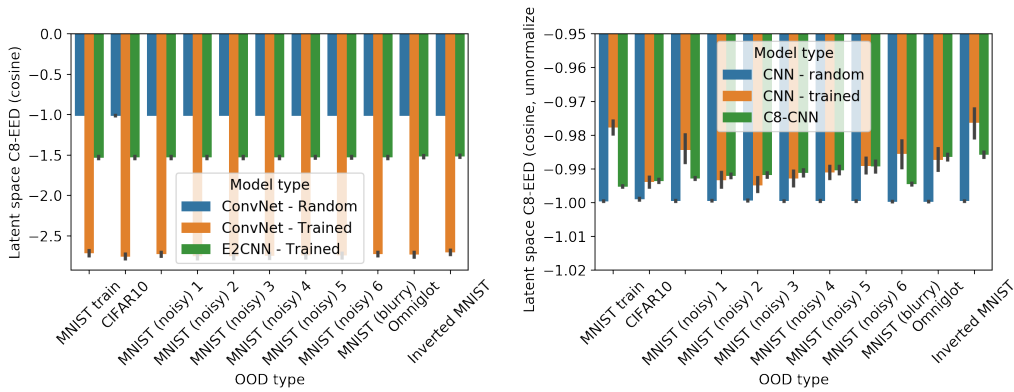


Figure 9: The cosine similarity version of latent space C_8 -EED (**normalized on the left, unnormalized on the right**) for conventional untrained CNNs, conventional CNNs trained on MNIST, and C_8 -equivariant CNNs (C_8 -CNN) [45] trained on MNIST with respect to a range of in- and out-of-distribution datasets. Both plots include 95% confidence intervals. **Lower values indicate more C_8 -invariance.** As can be seen, without normalization, the trained conventional CNNs and the C_8 -CNNs are often comparable. On the other hand, after normalization the conventional CNNs show much lower latent space C_8 -EED, indicating more C_8 -invariance. The differences between these two plots seems to indicate that the conventional CNNs have learned to better separate orbits of points rather than learning to cluster orbits together more tightly.

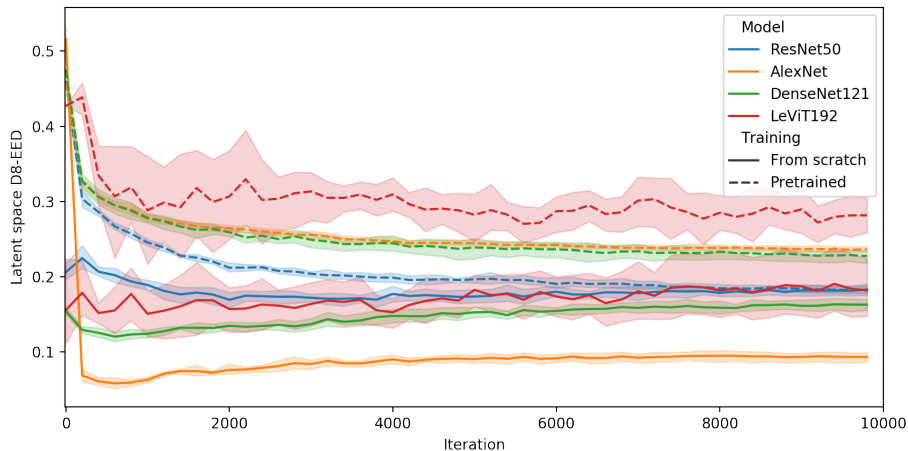


Figure 10: The latent space D_8 -EED measured every 200 training iterations (for a total of 10,000 iterations) for a range of model architectures that were initialized with either random or pretrained weights generated using ImageNet. Note that D_8 is the dihedral group of order 16 generated by a 45° angle and a reflection across an axis.

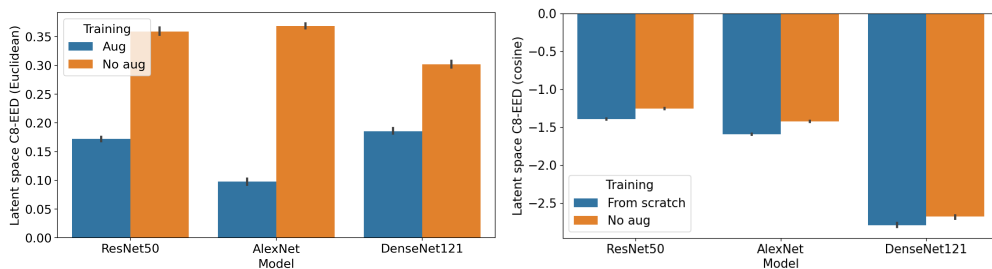


Figure 11: Latent space C_8 -EED on xView Maritime for models trained with and without rotation augmentation. **(Left)** The standard latent space C_8 -EED metric. **(Right)** The alternative version of latent space C_8 -EED where cosine similarity is used instead of Euclidean distance. Note that different models are not necessarily comparable since their latent spaces can have different dimension. **(smaller means more invariant to rotation.)**

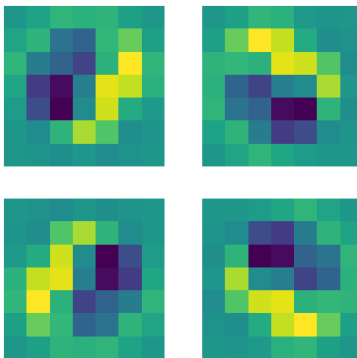


Figure 12: Four 7×7 filters from a randomly initialized C_4 -equivariant convolutional layer. Note that this is the orbit of one of these filters under the rotation action of C_4 .

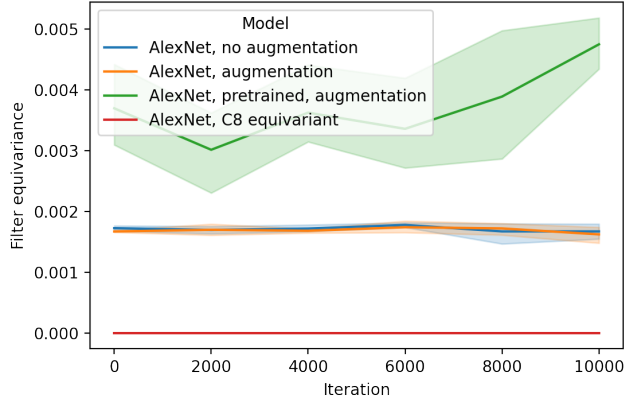


Figure 13: The average minimum ℓ_2 norm differences (7), between pairs of individual filters (one with group element $g \in C_4$ applied and one not) from the convolutional layer of AlexNets. Augmented training does not appear to cause emergent equivariance of the kind seen in hardcoded equivariant architecture.

AlexNet models trained on MNIST: AlexNet trained from scratch without rotation augmentation, AlexNet trained rotation augmentation but no pretraining, AlexNet with both pretraining and rotation augmentation, and finally Alex with C_8 -equivariant layers [45]. Random i and t are selected for each computation, and for computational simplicity we only evaluated on the subgroup C_4 of C_8 generated by 90-degree rotations.

A network where some filters are rotations of others would be expected to achieve a value of 0 for (7). Indeed, we can see that this is what happens to the C_8 -equivariant network. We see that the other networks do not achieve zero. Indeed, with the exception of the pretrained AlexNet, for which (7) increases slightly over training, the other non-equivariant networks do not change significantly at all. This indicates that this form of emergent equivariance does not emerge in this example.

A.5 A Proof of Proposition 3.1

Proof. 1. To prove this, consider the function $f : \mathbb{R}^2 \rightarrow \mathbb{R}$ defined such that for $(x, y) \in \mathbb{R}^2$

$$f(x, y) = \frac{x + y}{2}.$$

The order 2 cyclic group $\mathbb{Z}_2 = \{1, \sigma\}$ acts on \mathbb{R}^2 by permuting coordinates. That is, the only nonidentity element σ acts on \mathbb{R}^2 by sending $(x, y) \mapsto (y, x)$. It is clear that f is \mathbb{Z}_2 -invariant.

However, note that if $f_1 : \mathbb{R}^2 \rightarrow \mathbb{R}^2$ is defined by $f_1(x, y) = (2x, y)$ and $f_2 : \mathbb{R}^2 \rightarrow \mathbb{R}$ is defined by

$$f_2(x, y) = \frac{x + 2y}{4},$$

then $f = f_2 \circ f_1$. But neither f_1 nor f_2 is \mathbb{Z}_2 -equivariant to the actions described above.

2. This proof follows easily from the definitions. Suppose that f_1 is G -invariant, then for any $x \in X$ and $g \in G$, $f_1(gx) = f_1(x)$. Hence

$$f(gx) = f_2(f_1(gx)) = f_2(f_1(x)) = f(x).$$

□

A.6 A Proof of Proposition 3.2

Proof. First note that for fixed x and g , $m(f(gx), g\hat{f}(x)) = 0$ if and only if $f(gx) = gf(x)$. This follows from the fact that since G acts faithfully on Y , $\hat{f}(x) = f(x)$ and from the fact that m is

a metric. First assume that $m(f(gx), g\hat{f}(x)) = 0$. Then, since m is a metric, $f(gx) = g\hat{f}(x) = gf(x)$ giving the desired result. Next, if $f(gx) = gf(x) = g\hat{f}(x)$, then it again follows that $m(f(gx), g\hat{f}(x)) = 0$.

Next we recall the basic fact [17, proposition 2.16] from measure theory, which states that if $h : W \rightarrow [0, \infty]$ is a non-negative measurable function on measure space (W, ν) , then

$$\int_W h = 0 \Leftrightarrow h = 0 \text{ almost everywhere.} \quad (8)$$

Since $\hat{f}(x) = f(x)$, let $W = X \times G$ with $\xi = \nu \times \mu$ be the product measure on W generated by Haar measure μ on G , and the probability measure ν associated with \mathcal{D} . Note that f is measurable by virtue of being continuous, G acts linearly and hence is measurable, and m is measurable by virtue of being a metric. It follows that the function $h : X \times G \rightarrow [0, \infty]$ defined by

$$h(x, g) = m(f(gx), gf(x))$$

is measurable. The result then follows from the observation that m is non-negative (and hence h is) and from (8). That is, if (3) is zero, then since $m(f(gx), g\hat{f}(x))$ is non-negative, then (8) tells us that $m(f(gx), g\hat{f}(x))$ is zero almost-everywhere with respect to measure ξ . On the other hand, (8) also says that if $m(f(gx), g\hat{f}(x))$ is zero almost everywhere (including the case where this term is zero everywhere), then (3) is equal to zero. \square

A.7 The Reason for Normalization of Latent Space G -EED

We normalize $\mathcal{E}_{\text{latent}}(f, G)$ by M because when we use ℓ_2 -distance to compute G -EED without normalization, it is sensitive to scaling in a way that is unrelated to downstream task performance. To illustrate, note that if $f = f_2 \circ f_1$ is a model with feature extractor f_1 and classifier f_2 , then by scaling f_1 by $c > 1$, the unnormalized latent space G -EED increases, indicating a decrease in G -invariance. More precisely, if $f'_1 = cf_1$, then $\mathcal{E}(f'_1, G) = c\mathcal{E}(f_1, G)$. However, if we set $f'_2 = \frac{1}{c}f_2$, then $f'_2 \circ f'_1 = f = f_2 \circ f_1$. Thus, f_1 can be made to have arbitrarily large unnormalized latent space G -EED while the model f itself remains constant. A different but equally illustrative example is visualized in Figure 14. Two feature extractors have identical unnormalized latent space C_8 -EED for a single rotation orbit of an image of a 4 (average distance between blue points and their centroid), but the second feature extractor closely clusters points in the orbit relative to other instances from MNIST, while the first feature extractor does not. We would argue that in most cases the second feature extractor should be called *more invariant* with respect to this particular task. Normalization mitigates this issue, giving a more reasonable notion of latent space invariance in the context of machine learning.

A.8 Channelwise C_8 -EED for out-of-distribution datasets

In this section we provide Figure 15, which shows the channelwise C_8 -EED for collections of: CNN models with random weights, CNN models that have been trained on MNIST, and C_8 -CNN models that have been trained on MNIST.

In Figure 15 we show the channelwise C_8 -EED at layers 2 and 5 for each of the model types. Unsurprisingly, the C_8 -CNN has high C_8 -equivariance for all layers, whereas both the trained and untrained CNNs have substantially lower C_8 -equivariance. Across layers, the channelwise C_8 -EED remains fairly constant across datasets for the untrained models. However, the channelwise C_8 -EED for early layers of the trained CNNs differs across datasets (with equivariance on OOD datasets generally being less than the equivariance on the training set MNIST). In later layers, however, the difference in C_8 -equivariance between MNIST and an OOD dataset is negligible (Figure 15, right). This suggests that CNNs do learn some minimal amount of equivariance at early layers, but this equivariance either dissipates or becomes undetectable at later layers. Equivariance in earlier layers is also tied to image content. Images with high frequency signals tend to differ more significantly when rotated (with at the extreme end, a constant valued image unchanged with rotation).

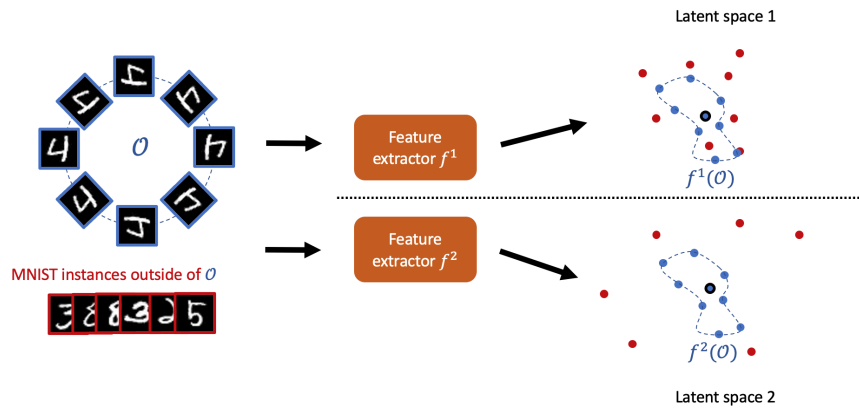


Figure 14: This illustration shows why it is important to normalize the latent space G -EED by the average distance between random pairs from the dataset. The set \mathcal{O} (blue) is the orbit of an image of a ‘4’ under the rotation action of C_8 . Two feature extractors f^1 and f^2 map \mathcal{O} as well as other unrelated images (red) from MNIST [14] to a latent space. While points from $f^1(\mathcal{O})$ and $f^2(\mathcal{O})$ both have the same average distance to their centroid, $f^2(\mathcal{O})$ clusters closely together relative to other points from the dataset. $f^1(\mathcal{O})$ is mixed with instances not belonging to $f^1(\mathcal{O})$. We would argue that f^2 extracts more invariant features.

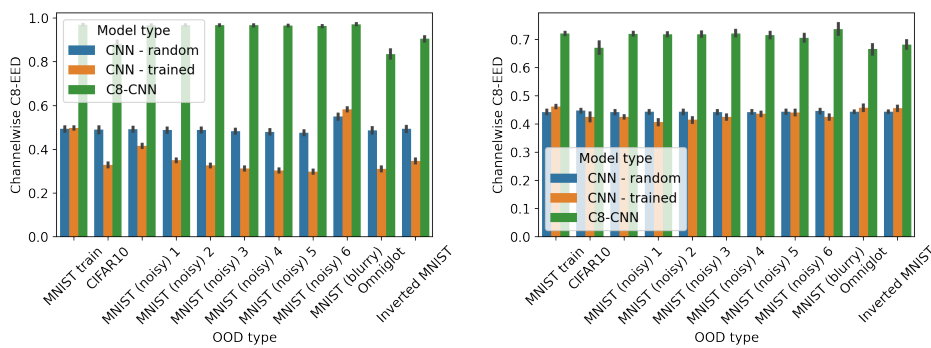


Figure 15: The channelwise C_8 -EED for the first two (left) and first five (right) convolutional blocks of a CNN with random weights, a CNN with weights trained on MNIST, and a C_8 -CNN with weights trained on MNIST. Error bars indicated 95% confidence intervals.

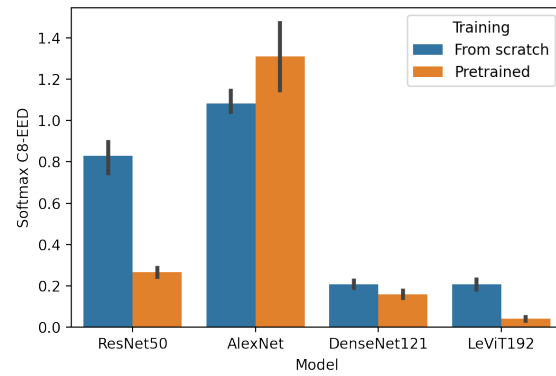


Figure 16: The softmax C_8 -EED after 10,000 iterations of training on xView maritime for a range of model architectures initialized with either random or pretrained weights generated using ImageNet. The 95% confidence intervals are represented by the black bars.